Catalysis Letters Vol. 73, No. 2-4, 2001

Synthesis of Fe-MCM-48 and its catalytic performance in phenol hydroxylation

Wei Zhao, Yunfei Luo, Peng Deng and Quanzhi Li *

Department of Chemistry, Fudan University, Shanghai 200433, PR China
E-mail: qzli @Fudan.edu.cn

Received 18 October 2000; accepted 6 March 2001

Highly ordered Fe-MCM-48 was synthesized by a mixed templation method under low molar ratio (0.17 : 1) of mixed surfactants to silica and characterized by XRD, ^{29}Si-MAS NMR, ESR, and UV-Visible. Its catalytic activity and selectivity was studied for phenol hydroxylation using H_2O_2 (30%). The substituting element (Fe^{3+}) is partially incorporated into the framework position forming a new type of active site which raises the phenol conversion to 43.6% and the diphenol (the mixture of catechol (CAT) and hydroquinone (HQ)) selectivity to 97.7%.

KEY WORDS: mesoporous molecular; Fe-MCM-48; mixed templation; phenol hydroxylation

1. Introduction

Diphenol production through phenol hydroxylation has been a hot research field since the 1970s [1,2]. Especially, after TS-1 [3] and TS-2 [4] appeared, the technology of this reaction has been greatly improved, and this reaction can be accomplished under mild conditions with good yields and selectivity. However, because of the limited pore size of these catalysts, which makes diffusion of substrates and products through the narrow channel of the microporous molecular sieves difficult, the conversion of phenol could not be enhanced obviously [5]. In the beginning of the 1990s, a new family of ordered mesoporous silicates of the M41s family was discovered and immediately received much attention because of its regular arrays of uniform channels and high surface area [6]. The features of these mesoporous materials are suitable for the larger molecular reaction and overcome the insufficiency described above for TS-1 and TS-2. Beside this, the synthesis of mesoporous silicas containing transition metals is much cheaper than the synthesis of TS-zeolites. Among the M41s family, MCM-48 characterized by a three-dimensional channel system may have several advantages over MCM-41 with a one-dimensional pore system when applied to catalytic reaction [7]. We all know that Fe^{3+} ions are very sensitive to oxidation–reduction reaction, so incorporating Fe^{3+} ions into the framework of cubic MCM-48 may result in a good potential catalyst for oxidation reactions. Up to now, by our knowledge there has not been any report of Fe-MCM-48 used as catalyst in an oxidation reaction. Because Si,Al-MCM-48 have been easily synthesized by the method of mixed templating of cationic–anionic surfactant in our laboratory [8,9], we used this method to prepare Fe-MCM-48 and then studied its catalytic performance in the phenol hydroxylation reaction.

2. Experimental

2.1. Synthesis and characterization

The synthesis mixture of Fe-MCM-48 was prepared as follows: tetraethylorthosilicate (TEOS) and an Fe source ($Fe_2(SO_4)_3 \cdot xH_2O$, MW 399.87) were added to the mixture solution of cetyltrimethylammonium bromide ($C_{16}H_{33}Me_3NBr$, CTAB), sodium laurate ($C_{11}H_{23}COONa$, SL), NaOH and H_2O. The molar composition of this mixture was 1.0 SiO_2 : 0.002–0.003 Fe_2O_3 : 0.153 CTAB : 0.017 SL : 0.25 NaOH : 100 H_2O (the molar composition of Si-MCM-48 is the same as described above except leaving out Fe_2O_3). Then this solution was stirred at 303 K for 1 h. After that, the mixture was placed in a static autoclave at 373 K for 4 days. The solid product was recovered and calcined, as described by Beck et al. [10]. All the samples were systematically characterized by powder X-ray diffraction (XRD, Rigaku D/Max-II A), ^{29}Si-MAS NMR (Bruker MSL-300), diffuse reflectance ultraviolet-visible (DRUV-Visible, Hitachi U-3410), and electron spin resonance (ESR, Bruker ER2000D-SRC).

2.2. Phenol hydroxylation

Phenol hydroxylation was carried out in a 50 ml glass reactor equipped with a thermometer, reflux condenser, tap funnel, and magnetic stirrer. Catalyst, phenol, and solvent were added successively into the reactor. The reaction was initiated by adding H_2O_2 (30 mass%) at the set temperature. The reaction conditions of this reaction are as follows: catalyst : phenol $= 1:10$ (mass ratio), phenol : $H_2O_2 = 1:1$ (molar ratio), $M_{H_2O_2} = 1$, H_2O as solvent, $T = 333$ K. Products were analyzed on a gas chromatograph using a flexible quartz capillary column coated with XE-60.

---

* To whom correspondence should be addressed.

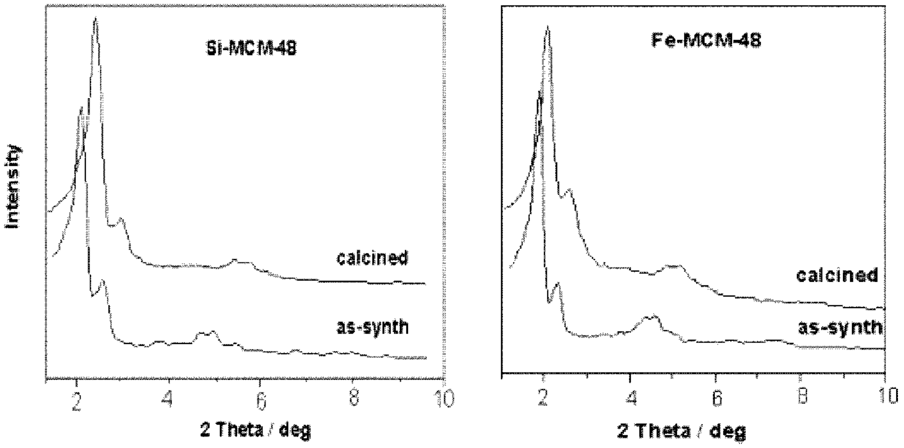

Figure 1. XRD pattern of Si- and Fe-MCM-48.

Table 1
XRD parameters of Fe-substituted MCM-48: d-value of reflection, constants of unit cell and unit cell shrinkage.

MCM-48	$d\{hkl\}$ (Å)				a_0[a]	Δ[b]
	{211}	{220}	{420}	{332}	(Å)	(%)
Si as-syn.	42.4	36.2	22.6	21.6	103.9	
Si calc.	37.2	31.4	20.1	19.2	91.1	12.3
Fe as-syn.	46.9	39.8	23.5	22.6	114.9	
Fe calc.	42.1	35.8	21.5	20.5	103.1	10.3

[a] $a_0 = d\{hkl\}\sqrt{(h^2+k^2+l^2)}$.
[b] Percent of unit cell shrinkage.

3. Results and discussion

3.1. XRD

The powder X-ray diffraction patterns of the Fe-substituted samples are shown in figure 1. The patterns are consistent with the pattern of MCM-48 reported in literature [11]. The position of the reflections and the values of cubic unit cell constants of Fe- and nonsubstituted siliceous MCM-48 before and after calcination are given in table 1. One can see that the a_0 of Fe-as-syn. is 11 Å greater than that of Si-as-syn. This suggests that some Fe^{3+} ions have been incorporated in the framework and caused the expansion of the unit cell. Calcination of the as-synthesized samples causes a shrinkage of about 10 or 12% of the unit cell for Fe-as-syn. or Si-as-syn., respectively.

3.2. Si-NMR

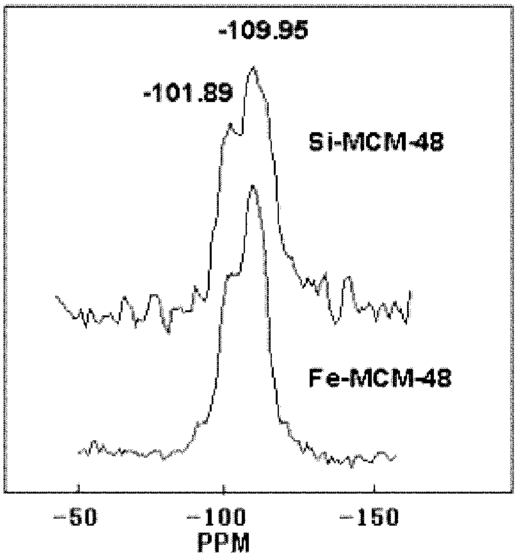

Figure 2. ^{29}Si MAS NMR spectra of calcined Si- and Fe-MCM-48.

Table 2
Connectivities of the framework of siliceous MCM-48 and Fe-MCM-48 samples determined by line deconvolution of ^{29}Si MAS NMR spectra.

MCM-48	Q^3 (%)	Q^4 (%)	Q^4/Q^3
Si calc.	20.5	79.5	3.89
Fe calc.	25.4	74.5	2.93

The ^{29}Si MAS NMR spectra of Si- and Fe-MCM-48 samples (figure 2) exhibit two lines with mean values of −101.89 and −109.95 ppm. They are assigned to $(SiO)_3$–SiOH (Q^3) or $Si(SiO)_4$ (Q^4) units, respectively [12]. The Q^4 portion of siliceous MCM-48 is somewhat higher than that of Fe-MCM-48 (table 2). This is probably due to steric constraints resulting from different size of the framework atoms and of the minimum inter-tetrahedral bond angles of the Si–O–Si and the Fe–O–Si bridge. Introducing substitution of Fe^{3+} ions into the framework should cause condensation within the framework to be more difficult, therefore decreasing framework connectivity (the decrease of Q^4) [13]. This is in agreement with the results of XRD.

3.3. ESR

The ESR spectra of the as-synthesized and calcined Fe-MCM-48 are shown in figure 3. With the as-synthesized Fe-MCM-48 sample, two main signals at $g = 2.06$ and at $g = 4.49$ (figure 3) were observed and are usually assigned to octahedrally and tetrahedrally coordinated isolated Fe^{3+} ions, respectively [14]. Upon thermal treatment in air, the

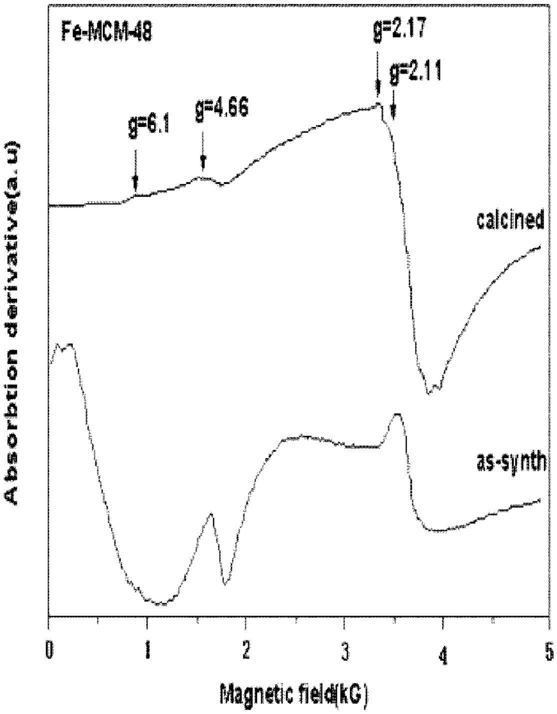

Figure 3. ESR spectra of as-synthesized and calcined Fe-MCM-48 ($T_{\mathrm{ESR}} =$ 298 K).

original signal at $g = 4.49$ is obviously decreased with shifting toward low field ($g = 4.66$) and new signals ($g = 2.11$, 2.17, and 6.1) appear. The signals at $g = 2.11$ and 2.17 are usually attributed to a non-framework Fe^{3+} species cluster [15], while the signal of $g = 6.1$ is commonly attributed to Fe^{3+} ions of the distorted tetrahedral or rhombohedrally distorted tetrahedral coordination [16]. The disappearance of the peak at $g = 2.06$ may be caused by two reasons: (1) Upon calcination, isolated octahedral Fe^{3+} ($g = 2.06$) partly changed into octahedral Fe^{3+} clusters ($g = 2.11$). (2) Because the intensity of the peak at $g = 2.17$ is much stronger than that of the peak at $g = 2.06$, the signal of the peak at $g = 2.06$ may be shielded. All of this shows that the Fe^{3+} ions have been incorporated into the framework of MCM-48, and the calcination results in the decrease and distortion of tetrahedrally coordinated Fe^{3+} ions in the framework.

3.4. UV-visible

There are two prominent absorption bands in the UV-visible spectra of as-synthesized Fe-MCM-48 (figure 4). The strong absorption in the 200–300 nm region (two clearly distinguished peaks at $\lambda = 212$ and 252 nm) attributed to the charge-transfer (CT) transitions involving isolated framework Fe^{3+} in $(FeO)_4^-$ tetrahedral geometry [17], and the weaker absorption in the 300–600 nm range (an obvious peak at $\lambda = 315$ nm) related with d–d transitions or octahedral Fe^{3+} present in small clusters [18,19]. Upon calcination, we observed: (i) the peak at 212 nm parallelly shifts towards higher wavelength; (ii) the peak at 252 nm splits off two peaks ($\lambda = 246$ and 270 nm); (iii) the peak at 315 nm is broadening and shifting toward higher wavelength ($\lambda = 325$ nm). The shift of the peak at 212 nm and the appearing of the peak at 246 nm show that the decrease and distortion of tetrahedral framework Fe^{3+} occur. The formation of an asymmetric peak at 270 nm suggests that part of the Fe^{3+} ions migrate from framework toward extraframework positions with formation of octahedral Fe^{3+} species [20], and the shift of the peak at 315 nm may be caused by the formation of superparamagnetic/ferromagnetic iron oxide clusters. This is in agreement with the results of ESR.

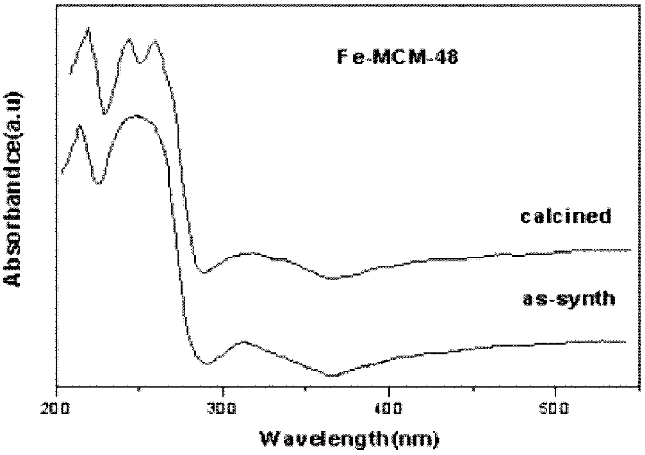

Figure 4. UV-visible spectra of as-synthesized and calcined Fe-MCM-48.

3.5. Phenol hydroxylation

The results of the phenol hydroxylation reaction show that Fe-MCM-48 has good catalytic activity (43.6%) and selectivity (97.7%) for this reaction and the catalytic performance of Fe-MCM-48 is obviously superior to that of TS-1 (table 3). The product distribution of this reaction on Fe-MCM-48 is different from that of Fe_2O_3 supported on MCM-48 (table 3, MCM-48 + $Fe_2(SO_4)_3$). It is worth mentioning that the selectivity of CAT in this reaction is very high (CAT/HQ = 3) on the Fe-MCM-48 catalyst. This shows that the active site of framework Fe^{3+} is different from that of extraframework Fe^{3+}; moreover, the electric and geometric arrangement of tetrahedrally coordinated framework Fe^{3+} can lead to the changing of the electric field environment in the inner channels of MCM-48, and then favorably yield good catalytic activity and high selectivity to CAT. Of course, with the increase of reaction time the secondary reactions (such as the further oxidation or polymerization of HQ) can also decrease the amount of HQ and then cause the enhancement of the CAT/HQ ratio. However, from table 4, we found that the process of secondary reactions is not obvious in this reaction and the product distribution only changes slightly with the increase of phenol conversion and the prolonging of reaction time. This suggests that the latter explanation is not the main reason for the high CAT/HQ ratio. Compared to Fe-MCM-41, Fe-MCM-48 has higher catalytic activity and nearly the same distribution of products for this reaction. This fact shows that the active centers of these two catalysts are similar and the cubic structure

Table 3
Catalytic activity comparison of various catalysts in the phenol hydroxylation.[a]

Catalyst	Conversion of phenol (%)	Distributions of products[b] (%)			
		CAT	HQ	Other	CAT/HQ
No catalyst	0.0	–	–	–	–
MCM-48	0.0	–	–	–	–
Fe_2O_3	13.3	57.5	30.9	11.6	1.9
MCM-48 + $Fe_2(SO_4)_3$[c]	30.2	61.5	28.9	9.6	2.1
Fe-MCM-48	43.6	73.3	24.4	2.3	3.0
Fe-MCM-41[d]	35.9	69.1	26.7	4.2	2.6
TS-1[e]	23.9	53.5	46.5	0	1.1

[a] Reaction time 4 h, temperature 333 K, reaction medium water, pH = 7.0, concentration of phenol 1.0 M, molar ratio phenol/H_2O_2 = 1.0, catalyst used 100 mg.
[b] CAT = catechol, HQ = hydroquinone, Other = unidentified products.
[c] Prepared by immersion method.
[d] Prepared by the same method as Fe-MCM-48.
[e] For TS-1: $m(\mathrm{TPAOH})/m(\mathrm{SiO_2}) = 0.2$.

Table 4
The effect of time on phenol hydroxylation.[a]

Time (h)	Conversion of phenol (%)	Distributions of products (%)			
		CAT	HQ	Other	CAT/HQ
1	31.8	72.3	25.9	1.8	2.8
2	37.5	72.7	25.3	2.0	2.9
4	43.6	73.3	24.4	2.3	3.0
6	40.4	73.1	24.1	2.8	3.0

[a] The reaction conditions are the same as in table 3.

of Fe-MCM-48 makes it more favorable than Fe-MCM-41 in material transmitting. This Fe-MCM-48 catalyst can be reused after the used samples are calcined to burn out the by-products covering some active centers during the reaction. When the Fe-MCM-48 was used in three runs to catalyze phenol hydroxylation, the phenol conversion was about 70% that in the first run. So the stability of Fe-MCM-48 remains to be improved.

4. Conclusion

Ordered mesoporous material Fe-MCM-48 was synthesized by the mixed templation method under low molar ratio (0.17 : 1) of mixed surfactants to silica and was characterized systematically. The results demonstrated that some Fe^{3+} ions have been successfully incorporated into the framework of MCM-48 and then cause the expansion of the unit cell and the decrease of framework connectivity. During the calcination, part of Fe^{3+} ions are removed from their framework positions to form extraframework species and the distortion of tetrahedrally coordinated framework isolated Fe^{3+} occurs. The active centers of framework isolated Fe^{3+} are favorable for phenol hydroxylation and have good selectivity for catechol.

Acknowledgement

This work is supported by NSFC under Project 29733070. CM9703942

References

[1] P. Maggioni, Ger. Offen. 2.314 (1974) 743.
[2] A.V. Eliseev, React. Kinet. Catal. Lett. 43 (1991) 419.
[3] M.G. Clerici, Appl. Catal. 68 (1991) 249.
[4] J.S. Reddy and S. Sivasanker, Catal. Lett. 11 (1991) 241.
[5] H. Norman, J. Coord. Chem. 19 (1988) 25.
[6] C.T. Kresge, M.E. Leanowicz and J.S. Beck, Nature 359 (1992) 710.
[7] K. Schumacher, Micropor. Mesopor. Mater. 27 (1999) 201.
[8] F. Chen, L. Huang and Q. Li, Chem. Mater. 9 (1997) 2685.
[9] F. Chen, F. Song and Q. Li, Micropor. Mesopor. Mater. 29 (1999) 305.
[10] J.S. Beck, J.C. Vartuli and J.L. Schleaker, J. Am. Chem. Soc. 114 (1992) 10834.
[11] V. Alfredsson and M.W. Anderson, Chem. Mater. 8 (1996) 1141.
[12] C.Y. Chen and M.E. Davis, Micropor. Mater. 2 (1993) 17.
[13] H. Kosslick and R. Fricke, J. Catal. 176 (1998) 102.
[14] L.E. Iton, B.R. Beal and D.T. Hodul, J. Mol. Catal. 21 (1983) 151.
[15] P. Selvam, S.K. Badamali and H. Kuwano, in: *Recent Trends in Catalysis*, eds. V. Murugesan, B. Arabindoo and M. Palanichamy (Narosa, New Delhi, 1999) p. 556.
[16] B.D. McNicol and D.T. Hodul, J. Catal. 25 (1972) 223.
[17] T. Inui, H. Nagata and M.J. Inoue, J. Catal. 139 (1993) 482.
[18] P. Ratnasamy and R. Kumar, Catal. Today 9 (1991) 341.
[19] R. Bongiovanni and D. Meisel, Chim. l'Indust. 4 (1994) 261.
[20] S. Bordiga, R. Buzzoni and G. Vlaic, J. Catal. 158 (1996) 486.